Tao Xu and Yong Chen*

Localised Nonlinear Waves in the Three-Component Coupled Hirota Equations

https://doi.org/10.1515/zna-2017-0264
Received July 29, 2017; accepted September 3, 2017

Abstract: We construct the Lax pair and Darboux transformation for the three-component coupled Hirota equations including higher-order effects such as third-order dispersion, self-steepening, and stimulated Raman scattering. A special vector solution of the Lax pair with 4×4 matrices for the three-component Hirota system is elaborately generated, based on this vector solution, various types of mixed higher-order localised waves are derived through the generalised Darboux transformation. Instead of considering various arrangements of the three potential functions q_1, q_2, and q_3, here, the same combination is considered as the same type solution. The first- and second-order localised waves are mainly discussed in six mixed types: (1) the hybrid solutions degenerate to the rational ones and three components are all rogue waves; (2) two components are hybrid solutions between rogue wave (RW) and breather (RW + breather), and one component is interactional solution between RW and dark soliton (RW + dark soliton); (3) two components are RW + dark soliton, and one component is RW + bright soliton; (4) two components are RW + breather, and one component is RW + bright soliton; (5) two components are RW + dark soliton, and one component is RW + bright soliton; (6) three components are all RW + breather. Moreover, these nonlinear localised waves merge with each other by increasing the absolute values of two free parameters α, β. These results further uncover some striking dynamic structures in the multicomponent coupled system.

Keywords: Breather and Soliton; Generalised Darboux Transformation; Localised Nonlinear Waves; Rogue Wave; Three-Component Coupled Hirota Equations.

***Corresponding author: Yong Chen,** Shanghai Key Laboratory of Trustworthy Computing, East China Normal University, Shanghai 200062, China; and Department of Physics, Zhejiang Normal University, Jinhua 321004, China, E-mail: ychen@sei.ecnu.edu.cn
Tao Xu: Shanghai Key Laboratory of Trustworthy Computing, East China Normal University, Shanghai 200062, China, E-mail: xutaohq@163.com

1 Introduction

In recent years, the semirational localised waves, which include bright or dark solitons, breathers, and rogue waves, have been one of the fascinating topics that have some potential applications in Bose–Einstein condenstates in atomic physics, optical fibers in nonlinear optics, and other fields. Rogue waves [1–4], (also called freak waves, monster waves, killer waves, or rabid-dog waves) have peak amplitude usually more than twice the significant wave height, and also appear from nowhere and disappear without a trace. Breathers propagate steadily and localise in either time or space, in particular, Akhmediev breather (AB) [5, 6] and Kuznetsov–Ma breather (KM) [7]. Akhmediev breathers are periodic in space and localise in time, whereas Kuznetsov–Ma breathers are periodic in time and localise in space. Interestingly, by taking the breathing period of the above two kinds of breathers to infinity, rogue waves localised in both time and space may be obtained. In 1983, Peregrine [8] first found a simple rational solution – the Peregrine soliton – which was the limiting case of the Kuznetsov–Ma breather and was especially considered as the rogue wave prototype [9].

There have been many articles on rogue waves and semirational localised waves of single-component systems, such as the nonlinear Schrödinger (NLS) equation [10–15], the derivative NLS equation [16–19], the Davey–Stewartson equation [20], the Hirota equation [21], the Kundu–Eckhaus equation [22], the complex short pulse equation [23], the Sasa–Satsuma equation [24], and so on. However, a variety of complex system, such as Bose–Einstein condensates and nonlinear optical fibers, usually involve more than one component [25–28]. Therefore, the discussion of localised waves in multicomponent coupled systems is greatly meaningful and necessary. Some different solutions of the mixed coupled NLS equation were classfied by Ling et al. [29]. The Maxwell–Bloch equtions [30] in two-level optical medium were solved to obtain breather, dark breather, rogue wave, and dark rogue waves. Meanwhile, performing the generalised Darboux transformation (DT) to the Maxwell–Bloch system, higher-order rogue waves, and W-shaped solitons were constructed by Wang and Liu [31].

Recently, the generalised DT was utilised to investigate higher-order rogue wave (RW) solutions of the NLS equation [11] and other nonlinear integrable systems [16, 22, 32, 33]. Baronio et al. [34] obtained first-order interactional solutions including the first-order RW, a dark or a bright soliton interacting with a first-order RW and a breather interacting with a first-order RW in the coupled NLS; however, the higher-order interactional solutions were not constructed. Besides, there have recently been various kinds of interactional solutions on different nonlinear models [35–37]. Bindu et al. [38], using the Painlevé analysis, dark soliton solutions were constructed in the two-component coupled Hirota equations, and multicomponent coupled Hirota system and its Lax pair were also constructed. In this article, enlightened by Baronio et al. [34] and Guo et al. [11], we investigate some novel higher-order localised wave solutions of the following three-component coupled Hirota equations from Bindu et al. [38] and Zhang and Yuan [39]

$$
\begin{aligned}
&iq_{1t}+\frac{1}{2}q_{1xx}+(|q_1|^2+|q_2|^2+|q_3|^2)q_1+i\epsilon[q_{1xxx}+3(2|q_1|^2+|q_2|^2+|q_3|^2)q_{1x}+3q_1(q_2^*q_{2x}+q_3^*q_{3x})]=0,\\
&iq_{2t}+\frac{1}{2}q_{2xx}+(|q_1|^2+|q_2|^2+|q_3|^2)q_2+i\epsilon[q_{2xxx}+3(2|q_2|^2+|q_1|^2+|q_3|^2)q_{2x}+3q_2(q_1^*q_{1x}+q_3^*q_{3x})]=0,\\
&iq_{3t}+\frac{1}{2}q_{3xx}+(|q_1|^2+|q_2|^2+|q_3|^2)q_3+i\epsilon[q_{3xxx}+3(2|q_3|^2+|q_1|^2+|q_3|^2)q_{3x}+3q_3(q_1^*q_{1x}+q_2^*q_{2x})]=0.
\end{aligned}
\tag{1}
$$

where $q_1(x, t)$, $q_2(x, t)$, and $q_3(x, t)$ are the complex envelops of three fields, each non-numeric subscripted variable stands for partial differentiation. Besides, q_i^* $(i=1, 2, 3)$ denotes the complex conjugation of q_i. ϵ stands for the integrable perturbation of the coupled NLS equation [40], which is a small dimensionless real parameter. In the regime of ultra-short pulses, where the pulse lengths become comparable with the wavelength [23, 41], the NLS equation becomes less accurate. To meet this requirement, one of the approaches is to add some higher-order dispersive terms [42] in the standard NLS equation. In this way, Tasgal and Potasek [43] presented the two-component coupled Hirota equations, including third-order dispersion, self-steepening, and stimulated Raman scattering. The coupled system (1) is an obvious three-component generalisation of the two-component coupled Hirota equations from Tasgal and Potasek [43] and Wang et al. [44], and it governs the simultaneous propagation of three fields in the normal dispersion regime of optical fibers. Through the binary DT, multidark solitons were constructed for the one-component and multicomponent Hirota systems in Zhang and Yuan [45] and Zhang and Yuan [39], respectively.

Using the generalised DT method, the higher-order localised waves including the second-order rogue waves interacting with two dark or bright solitons, the second-order rogue waves interacting with two paralleled breathers were generated in the coupled NLS equation [46], which generalised Baronio et al.'s work [34] into the higher-order case. Analogously, some novel higher-order localised wave solutions were constructed in the two-component coupled Hirota equations [46, 47] and the three-component coupled NLS equations [48]. Through considering both the two-component (even) [46] and the three-component (odd) coupled Hirota equations, the localised waves of the multicomponent coupled Hirota system may be well understood. Compared with the two-component Hirota equations, more free parameters exist in the expressions of localised wave solutions in the three-component Hirota system. Additionally, some abundant and interesting mixed interactional solutions will be constructed in the three-component Hirota system (1). Based on the above facts, it is very necessary to investigate the higher-order localised waves of the system (1).

Here, starting from the appropriate periodic seed solutions, a special vector solution of the Lax pair of the system (1) is elaborately constructed. Based on this kind of the special vector solution and the generalised DT, some abundant higher-order localised waves of the three-component Hirota equations are demonstrated. Among these higher-order localised waves, the first- and second-order ones are mainly classified in six mixed types: (1) the hybrid solutions degenerate to the rational ones and three components are all rogue waves; (2) two components are hybrid solutions between rogue wave (RW) and breather (RW + breather), and one component is interactional solution between RW and dark soliton (RW + dark soliton); (3) two components are RW + dark soliton, and one component is RW + bright soliton; (4) two components are RW + breather, and one component is RW + bright soliton; (5) two components are RW + dark soliton, and one component is RW + bright soliton; (6) three components are all RW + breather. Choosing the appropriate values of some free parameters in these semirational solutions, several interesting dynamics of the interactional solutions are exhibited. Besides, these above mixed interactional solutions can only be generated in the coupled systems, which are larger than two components.

The article is organised as follows. In Section 2, the generalised DT of the three-component coupled Hirota system is constructed. In Section 3, the first- and second-order localised waves are obtained, respectively, and some interesting and appealing figures are also given. The last section contains several conclusions and discussions.

2 Generalised DT

In this section, we construct the Lax pair with 4×4 matrixes and the generalised DT [11, 49] of the three-component coupled Hirota equations [38, 39] by making use of the Ablowitz–Kaup–Newell–Segur (AKNS) technique [50]. The Lax pair of the coupled system (1) can be constructed as follows:

$$\Phi_x = U\Phi = (\lambda U_0 + U_1)\Phi, \tag{2}$$

$$\Phi_t = V\Phi = (\lambda^3 V_0 + \lambda^2 V_1 + \lambda V_2 + V_3)\Phi, \tag{3}$$

where

$$U_0 = \frac{1}{12\epsilon}\begin{bmatrix} -2i & 0 & 0 & 0 \\ 0 & i & 0 & 0 \\ 0 & 0 & i & 0 \\ 0 & 0 & 0 & i \end{bmatrix}, \quad U_1 = \begin{bmatrix} 0 & -q_1 & -q_2 & -q_3 \\ q_1^* & 0 & 0 & 0 \\ q_2^* & 0 & 0 & 0 \\ q_3^* & 0 & 0 & 0 \end{bmatrix},$$

$$V_0 = \frac{1}{16\epsilon}U_0, \quad V_1 = \frac{1}{8\epsilon}U_0 + \frac{1}{16\epsilon}U_1,$$

$$V_2 = \frac{1}{4}\begin{bmatrix} ie & -\frac{q_1}{2\epsilon} - iq_{1x} & -\frac{q_2}{2\epsilon} - iq_{2x} & -\frac{q_3}{2\epsilon} - iq_{3x} \\ \frac{q_1^*}{2\epsilon} - iq_{1x}^* & -i|q_1|^2 & -iq_1^*q_2 & -iq_1^*q_3 \\ \frac{q_2^*}{2\epsilon} - iq_{2x}^* & -iq_2^*q_1 & -i|q_2|^2 & -iq_2^*q_3 \\ \frac{q_3^*}{2\epsilon} - iq_{3x}^* & -iq_3^*q_1 & -iq_3^*q_2 & -i|q_3|^2 \end{bmatrix},$$

$$V_3 = \begin{bmatrix} \epsilon(e_1+e_2+e_3) + \frac{i}{2}e & \epsilon e_4 - \frac{i}{2}q_{1x} & \epsilon e_5 - \frac{i}{2}q_{2x} & \epsilon e_6 - \frac{i}{2}q_{3x} \\ -\epsilon e_4^* - \frac{i}{2}q_{1x}^* & -\epsilon e_1 - \frac{i}{2}|q_1|^2 & \epsilon e_7 - \frac{i}{2}q_1^*q_2 & \epsilon e_8 - \frac{i}{2}q_1^*q_3 \\ -\epsilon e_5^* - \frac{i}{2}q_{2x}^* & -\epsilon e_7^* - \frac{i}{2}q_2^*q_1 & -\epsilon e_2 - \frac{i}{2}|q_2|^2 & \epsilon e_9 - \frac{i}{2}q_2^*q_3 \\ -\epsilon e_6^* - \frac{i}{2}q_{3x}^* & -\epsilon e_8^* - \frac{i}{2}q_3^*q_1 & -\epsilon e_9^* - \frac{i}{2}q_3^*q_2 & -\epsilon e_3 - \frac{i}{2}|q_3|^2 \end{bmatrix},$$

with

$$e = |q_1|^2 + |q_2|^2 + |q_3|^2, \quad e_1 = q_1q_{1x}^* - q_{1x}q_1^*,$$
$$e_2 = q_2q_{2x}^* - q_{2x}q_2^*, \quad e_3 = q_3q_{3x}^* - q_{3x}q_3^*, \quad e_4 = q_{1xx} + 2eq_1,$$
$$e_5 = q_{2xx} + 2eq_2, \quad e_6 = q_{3xx} + 2eq_3, \quad e_7 = q_1^*q_{2x} - q_{1x}^*q_2,$$
$$e_8 = q_1^*q_{3x} - q_{1x}^*q_3, \quad e_9 = q_2^*q_{3x} - q_{2x}^*q_3.$$

Here, the column vector $\Phi = (\phi, \varphi, \chi, \psi)^T$ is the eigenfunction of the Lax pair (2–3). Actually, the three-component coupled Hirota system (1) can be straightforwardly derived by the following compatibility condition $U_t - V_x + [U, V] = 0$.

The Lax pair of (1) is the standard AKNS spectral problem, based on the DT of AKNS [49, 51] hierarchy, the generalised DT of (1) could be directly constructed. However, U and V are all 4×4 matrices in the Lax pair (2–3), it is more complicated than 2×2 and 3×3 matrix spectral problems to construct the specific vector solution of the corresponding Lax pair.

Let $\Phi_1 = (\phi_1, \varphi_1, \chi_1, \psi_1)^T$ be a special solution of Lax pair (2–3) at $q_1 = q_1[0]$, $q_2 = q_2[0]$, $q_3 = q_3[0]$ and $\lambda = \lambda_1$. Then, we can get the following classic DT of the three-component coupled Hirota equations (1)

$$\Phi_1 = T[1]\Phi,$$
$$T[1] = \lambda I - H[0]\Lambda_1 H[0] = (\lambda - \lambda_1^*)I + (\lambda_1^* - \lambda_1)\frac{\Phi_1[0]\Phi_1[0]^\dagger}{\Phi_1[0]^\dagger\Phi_1[0]}, \tag{4}$$

$$q_1[1] = q_1[0] + i(\lambda_1 - \lambda_1^*)\frac{\phi_1[0]\varphi_1[0]^*}{4\epsilon(|\phi_1[0]|^2 + |\varphi_1[0]|^2 + |\chi_1[0]|^2 + |\psi_1[0]|^2)}, \tag{5}$$

$$q_2[1] = q_2[0] + i(\lambda_1 - \lambda_1^*)\frac{\phi_1[0]\chi_1[0]^*}{4\epsilon(|\phi_1[0]|^2 + |\varphi_1[0]|^2 + |\chi_1[0]|^2 + |\psi_1[0]|^2)}, \tag{6}$$

$$q_3[1] = q_3[0] + i(\lambda_1 - \lambda_1^*)\frac{\phi_1[0]\psi_1[0]^*}{4\epsilon(|\phi_1[0]|^2 + |\varphi_1[0]|^2 + |\chi_1[0]|^2 + |\psi_1[0]|^2)}, \tag{7}$$

where $(\phi_1[0], \varphi_1[0], \chi_1[0], \psi_1[0])^T = (\phi_1, \varphi_1, \chi_1, \psi_1)^T$, † denotes transposed and conjugate operation of a vector and I admits the 4×4 identity matrix,

$$H[0] = \begin{bmatrix} \phi_1[0] & \varphi_1[0]^* & \psi_1[0]^* & 0 \\ \varphi_1[0] & -\phi_1[0]^* & 0 & 0 \\ \chi_1[0] & 0 & 0 & \psi_1[0]^* \\ \psi_1[0] & 0 & -\phi_1[0]^* & -\chi_1[0]^* \end{bmatrix},$$
$$\Lambda_1 = \begin{bmatrix} \lambda_1 & 0 & 0 & 0 \\ 0 & \lambda_1^* & 0 & 0 \\ 0 & 0 & \lambda_1^* & 0 \\ 0 & 0 & 0 & \lambda_1^* \end{bmatrix}. \tag{8}$$

According to the above classic DT (4–7), the generalised DT can be constructed in the following content. Setting

$\Phi_1=(\phi_1,\ \varphi_1,\ \chi_1,\ \psi_1)^T=\Phi_1(\lambda_1+\delta)$ as a special solution of the Lax pair (2–3) with $q_1=q_1[0]$, $q_2=q_2[0]$, $q_3=q_3[0]$ and $\lambda=\lambda_1+\delta$, then the eigenfunction Φ_1 can be expanded as the Taylor series at $\delta=0$

$$\Phi_1=\Phi_1^{[0]}+\Phi_1^{[1]}\delta+\Phi_1^{[2]}\delta^2+\cdots+\Phi_1^{[N]}\delta^N+\cdots, \tag{9}$$

where

$$\Phi_1^{[l]}=(\phi_1^{[l]},\ \varphi_1^{[l]},\ \chi_1^{[l]},\ \psi_1^{[l]})^T,$$
$$\Phi_1^{[l]}=\frac{1}{l!}\frac{\partial^l\Phi_1}{\partial\delta^l}\Big|_{\delta=0}\quad (l=0,\ 1,\ 2,\ 3\cdots).$$

It can be easily found out that $\Phi_1[0]=\Phi_1^{[0]}$ is a particular solution of the Lax pair (2–3) with $q_1=q_1[0]$, $q_2=q_2[0]$, $q_3=q_3[0]$, and $\lambda=\lambda_1$. From the above process, we can directly give the first-step generalised DT.

2.1 The First-Step Generalised DT

$$\Phi_1=T[1]\Phi,\quad T[1]=\lambda I-H[0]\Lambda_1H[0]^{-1}, \tag{10}$$

$$q_1[1]=q_1[0]+i(\lambda_1-\lambda_1^*)\frac{\phi_1[0]\varphi_1[0]^*}{4\epsilon(|\phi_1[0]|^2+|\varphi_1[0]|^2+|\chi_1[0]|^2+|\psi_1[0]|^2)}, \tag{11}$$

$$q_2[1]=q_2[0]+i(\lambda_1-\lambda_1^*)\frac{\phi_1[0]\chi_1[0]^*}{4\epsilon(|\phi_1[0]|^2+|\varphi_1[0]|^2+|\chi_1[0]|^2+|\psi_1[0]|^2)}, \tag{12}$$

$$q_3[1]=q_3[0]+i(\lambda_1-\lambda_1^*)\frac{\phi_1[0]\psi_1[0]^*}{4\epsilon(|\phi_1[0]|^2+|\varphi_1[0]|^2+|\chi_1[0]|^2+|\psi_1[0]|^2)}, \tag{13}$$

where $\Phi_1[0]=\Phi_1^{[0]}=(\phi_1[0],\ \varphi_1[0],\ \chi_1[0],\ \psi_1[0])^T$. Meanwhile, the explicit expressions of $H[0]$ and Λ_1 are given in (8).

2.2 The Second-Step Generalised DT

Choosing the seed solution of the three-component coupled Hirota equations (1) as $q_1=q_1[1]$, $q_2=q_2[1]$, $q_3=q_3[1]$ at $\lambda=\lambda_1+\delta$, then $T[1]\Phi_1$ is the solution of the Lax pair (2–3). We take into account the following limit:

$$\lim_{\delta\to 0}\frac{T[1]|_{\lambda=\lambda_1+\delta}\,\Phi_1}{\delta}=\lim_{\delta\to 0}\frac{(\delta+T_1[1])\Phi_1}{\delta}=\Phi_1^{[0]}+T_1[1]\Phi_1^{[1]}\equiv\Phi_1[1].$$

The second-step generalised DT can be expressed as follows:

$$\Phi_2=T[2]T[1]\Phi,\quad T[2]=\lambda I-H[1]\Lambda_2H[1]^{-1}, \tag{14}$$

$$q_1[2]=q_1[1]+i(\lambda_1-\lambda_1^*)\frac{\phi_1[1]\varphi_1[1]^*}{4\epsilon(|\phi_1[1]|^2+|\varphi_1[1]|^2+|\chi_1[1]|^2+|\psi_1[1]|^2)}, \tag{15}$$

$$q_2[2]=q_2[1]+i(\lambda_1-\lambda_1^*)\frac{\phi_1[1]\chi_1[1]^*}{4\epsilon(|\phi_1[1]|^2+|\varphi_1[1]|^2+|\chi_1[1]|^2+|\psi_1[1]|^2)}, \tag{16}$$

$$q_3[2]=q_3[1]+i(\lambda_1-\lambda_1^*)\frac{\phi_1[1]\psi_1[1]^*}{4\epsilon(|\phi_1[1]|^2+|\varphi_1[1]|^2+|\chi_1[1]|^2+|\psi_1[1]|^2)}, \tag{17}$$

where $\Phi_1[1]=(\phi_1[1],\ \varphi_1[1],\ \chi_1[1],\ \psi_1[1])^T$, $\Lambda_2=\Lambda_1$ and $T_1[1]=\lambda_1I-H[0]\Lambda_1H[0]^{-1}$,

$$H[1]=\begin{bmatrix}\phi_1[1] & \varphi_1[1]^* & \psi_1[1]^* & 0\\ \varphi_1[1] & -\phi_1[1]^* & 0 & 0\\ \chi_1[1] & 0 & 0 & \psi_1[1]^*\\ \psi_1[1] & 0 & -\phi_1[1]^* & -\chi_1[1]^*\end{bmatrix}.$$

2.3 The Third-Step Generalised DT

In a similar way, the following limit will be constructed:

$$\lim_{\delta\to 0}\frac{(T[2]T[1])|_{\lambda=\lambda_1+\delta}\,\Phi_1}{\delta^2}=\lim_{\delta\to 0}\frac{(\delta+T_1[2])(\delta+T_1[1])\Phi_1}{\delta^2}$$
$$=\Phi_1^{[0]}+(T_1[1]+T_1[2])\Phi_1^{[1]}+T_1[2]T_1[1]\Phi_1^{[2]}\equiv\Phi_1[2],$$

the eigenfunction $\Phi_1[2]$ is the specific solution of the Lax pair (2–3) at $q_1=q_1[2]$, $q_2=q_2[2]$, $q_3[2]$, and $\lambda=\lambda_1$. Additionally, the following two identities

$$T_1[1]\Phi_1^{[0]}=0,\qquad T_1[2](\Phi_1^{[0]}+T_1[1]\Phi_1^{[1]})=0,$$

have been utilised in the above process.

The third-step generalised DT can be generated as

$$\Phi_3=T[3]T[2]T[1]\Phi,\quad T[3]=\lambda I-H[2]\Lambda_3H[2]^{-1}, \tag{18}$$

$$q_1[3]=q_1[2]+i(\lambda_1-\lambda_1^*)\frac{\phi_1[2]\varphi_1[2]^*}{4\epsilon(|\phi_1[2]|^2+|\varphi_1[2]|^2+|\chi_1[2]|^2+|\psi_1[2]|^2)}, \tag{19}$$

$$q_2[3]=q_2[2]+i(\lambda_1-\lambda_1^*)\frac{\phi_1[2]\chi_1[2]^*}{4\epsilon(|\phi_1[2]|^2+|\varphi_1[2]|^2+|\chi_1[2]|^2+|\psi_1[2]|^2)},\tag{20}$$

$$q_3[3]=q_3[2]+i(\lambda_1-\lambda_1^*)\frac{\phi_1[2]\psi_1[2]^*}{4\epsilon(|\phi_1[2]|^2+|\varphi_1[2]|^2+|\chi_1[2]|^2+|\psi_1[2]|^2)},\tag{21}$$

where $\Phi_1[2]=(\phi_1[2],\ \varphi_1[2],\ \chi_1[2],\ \psi_1[2])^T$, $\Lambda_3=\Lambda_1$ and $T_1[2]=\lambda_1 I-H[1]\Lambda_2 H[1]^{-1}$,

$$H[2]=\begin{bmatrix}\phi_1[2] & \varphi_1[2]^* & \psi_1[2]^* & 0\\ \varphi_1[2] & -\phi_1[2]^* & 0 & 0\\ \chi_1[2] & 0 & 0 & \psi_1[2]^*\\ \psi_1[2] & 0 & -\phi_1[2]^* & -\chi_1[2]^*\end{bmatrix}.$$

2.4 The *N*-Step Generalised DT

Iterating the above procedures, the N-step generalised DT of the three-component coupled Hirota equations (1) can be derived as follows:

$$\Phi[N]=T[N]T[N-1]\cdots T[1]\Phi,$$
$$T[N]=\lambda I-H[N-1]\Lambda_N H[N-1]^{-1},\tag{22}$$

$$\Phi_1[N-1]=\Phi_1^{[0]}+\sum_{l=1}^{N-1}T_1[l]\Phi_1^{[1]}+\sum_{l=1}^{N-1}\sum_{k=1}^{l-1}T_1[l]T_1[k]\Phi_1^{[2]}+\cdots$$
$$+T_1[N-1]T_1[N-2]\tag{23}$$
$$\cdots T_1[1]\Phi_1^{[N-1]},\tag{24}$$

$$q_1[N]=q_1[N-1]+\frac{i(\lambda_1-\lambda_1^*)\phi_N[N-1]\varphi_N[N-1]^*}{4\epsilon(|\phi_N[N-1]|^2+|\varphi_N[N-1]|^2+|\chi_N[N-1]|^2+|\psi_N[N-1]|^2)},\tag{25}$$

$$q_2[N]=q_2[N-1]+\frac{i(\lambda_1-\lambda_1^*)\phi_N[N-1]\chi_N[N-1]^*}{4\epsilon(|\phi_N[N-1]|^2+|\varphi_N[N-1]|^2+|\chi_N[N-1]|^2+|\psi_N[N-1]|^2)},\tag{26}$$

$$q_3[N]=q_3[N-1]+\frac{i(\lambda_1-\lambda_1^*)\phi_N[N-1]\psi_N[N-1]^*}{4\epsilon(|\phi_N[N-1]|^2+|\varphi_N[N-1]|^2+|\chi_N[N-1]|^2+|\psi_N[N-1]|^2)},\tag{27}$$

where

$$H[l-1]=\begin{bmatrix}\phi_1[l-1] & \varphi_1[l-1]^* & \psi_1[l-1]^* & 0\\ \varphi_1[l-1] & -\phi_1[l-1]^* & 0 & 0\\ \chi_1[l-1] & 0 & 0 & \psi_1[l-1]^*\\ \psi_1[l-1] & 0 & -\phi_1[l-1]^* & -\chi_1[l-1]^*\end{bmatrix},$$

$$\Lambda_l=\begin{bmatrix}\lambda_1 & 0 & 0 & 0\\ 0 & \lambda_1^* & 0 & 0\\ 0 & 0 & \lambda_1^* & 0\\ 0 & 0 & 0 & \lambda_1^*\end{bmatrix}(1\le l\le N),$$

$\Phi_1[N-1]=(\phi_1[N-1],\ \varphi_1[N-1],\ \chi_1[N-1],\ \psi_1[N-1])^T\ (N\ge 1)$,
$T_1[l]=\lambda_1 I-H[l-1]\Lambda_l H[l-1]^{-1}$.

Furthermore, the Nth-order localised waves in the three-component coupled Hirota equations (1) can be generated through the formulae (22–27). To avoid calculating the determinant of higher order matrix in a cumbersome way, here, the iterative algorithm is chosen instead of Crum theorem [49]. Additionally, the calculations and expressions of the higher-order interactional solutions of the three-component coupled Hirota equations (1) are very complicated and tedious, so the first- and second-order localised wave solutions are discussed in detail.

3 Localised Nonlinear Wave Solutions

In this section, some novel mixed interactional solutions of the three-component coupled Hirota equations (1) are constructed through the above generalised DT. Here, the first- and second-order localised waves are discussed in detail and some figures of these kinds of localised wave solutions are also exhibited. Besides, some dynamic structures of these nonlinear waves are demonstrated.

3.1 The First-Order Localised Nonlinear Waves

We begin with the plane wave seed solutions of the coupled system (1) [44, 46, 48]

$$q_1[0]=d_1e^{i\theta},\qquad q_2[0]=d_2e^{i\theta},\qquad q_3[0]=d_3e^{i\theta},\tag{28}$$

where $\theta=(d_1^2+d_2^2+d_3^2)t$, d_1, d_2, d_3 are three arbitrary real constants, which delegate the amplitudes of the three continuous-wave backgrounds. Here, the expression $d_1^2+d_2^2+d_3^2$ refers to frequencies of the three continuous-wave backgrounds. Conveniently, the above seed solutions are chosen periodically in time variable t without depending on space variable x. Then, a special vector solution of the Lax pair (2–3) can be constructed with $q_1=q_1[0]$, $q_2=q_2[0]$, and $q_3=q_3[0]$ as follows:

$$\Phi_1=\begin{pmatrix} (c_1e^{M_1+M_2}-c_2e^{M_1-M_2})e^{\frac{i\theta}{2}} \\ \rho_1(c_2e^{M_1+M_2}-c_1e^{M_1-M_2})e^{-\frac{i\theta}{2}}-(\alpha d_2+\beta d_3)e^{M_3} \\ \rho_2(c_2e^{M_1+M_2}-c_1e^{M_1-M_2})e^{-\frac{i\theta}{2}}+\alpha d_1e^{M_3} \\ \rho_3(c_2e^{M_1+M_2}-c_1e^{M_1-M_2})e^{-\frac{i\theta}{2}}+\beta d_1e^{M_3} \end{pmatrix}, \tag{29}$$

where

$$c_1=\frac{\left(\lambda-\sqrt{\lambda^2+64\epsilon^2(d_1^2+d_2^2+d_3^2)}\right)^{\frac{1}{2}}}{\sqrt{\lambda^2+64\epsilon^2(d_1^2+d_2^2+d_3^2)}},$$

$$c_2=\frac{\left(\lambda+\sqrt{\lambda^2+64\epsilon^2(d_1^2+d_2^2+d_3^2)}\right)^{\frac{1}{2}}}{\sqrt{\lambda^2+64\epsilon^2(d_1^2+d_2^2+d_3^2)}},$$

$$\rho_1=\frac{d_1}{\sqrt{d_1^2+d_2^2+d_3^2}},\quad \rho_2=\frac{d_2}{\sqrt{d_1^2+d_2^2+d_3^2}},$$

$$\rho_3=\frac{d_3}{\sqrt{d_1^2+d_2^2+d_3^2}},\quad M_1=-\frac{i\lambda}{384\epsilon^2}[16\epsilon x+\lambda(\lambda+2)t],$$

$$M_3=\frac{i\lambda}{192\epsilon^2}[16\epsilon x+\lambda(\lambda+2)t],$$

$$M_2=\frac{i}{128\epsilon^2}\sqrt{\lambda^2+64\epsilon^2(d_1^2+d_2^2+d_3^2)}\Bigg[16\epsilon x+\lambda(\lambda+2)t$$
$$-32\epsilon^2(d_1^2+d_2^2+d_3^2)+\sum_{k=1}^{N}s_kf^{2k}\Bigg].$$

where $s_k=m_k+in_k$ $(1\le k\le N)$, m_k, n_k, α, and β are real free parameters and f is a small parameter. During the process of calculation of the special vector solution (29), the variable coefficient differential equations in the Lax pair (2–3) need to be converted into constant coefficient ones by a gauge transformation. Here, the transformed Lax pair can be written as $\phi_x=RU\phi$, $\phi_t=RV\phi$ and the characteristic equation of RU is a quartic equation. To construct some new patterns of interactional solutions of the coupled system (1), we consider that the characteristic equation of RU possesses two groups of double roots. Besides, the full solutions in the fundamental solution matrix of U are all included in (29), such as these expressions $-(\alpha d_2+\beta d_3)e^{M_3}$, $\alpha d_1e^{M_3}$ and $\beta d_1e^{M_3}$. When constructing the higher-order rogue wave solutions of the coupled system (1), the above expressions $-(\alpha d_2+\beta d_3)e^{M_3}$, $\alpha d_1e^{M_3}$, and $\beta d_1e^{M_3}$ are not needed. However, these expressions are greatly necessary to generate the interactional solutions of the three-component coupled Hirota system (1), especially the free parameters d_i $(i=1,\ 2,\ 3)$, α, β play a critical role in constructing different mixed hybrid solutions in the three potential functions q_1, q_2, and q_3. Setting $\tau=d_1^2+d_2^2+d_3^2$ and choosing the spectral parameter $\lambda=8i\sqrt{\tau}\epsilon(1+f^2)$, we can get the Taylor expansion of the vector function Φ_1 at $f=0$

$$\Phi_1(f)=\Phi_1^{[0]}+\Phi_1^{[1]}f^2+\Phi_1^{[2]}f^4+\Phi_1^{[3]}f^6+\cdots, \tag{30}$$

where $\Phi_1^{[k]}=(\phi_1^{[k]},\ \varphi_1^{[k]},\ \chi_1^{[k]},\ \psi_1^{[k]})^T=\dfrac{\partial^{2k}\Phi_1}{\partial f^{2k}}\Big|_{f=0}$ $(1\le k\le N)$,

$$\phi_1^{[0]}=\frac{(i-1)\left[2\sqrt{\tau}(x-6\tau\epsilon t)+2i\tau t+1\right]}{4\sqrt{\epsilon}\tau^{\frac{1}{4}}}e^{\xi_1},$$

$$\varphi_1^{[0]}=\frac{(i-1)d_1\left[2\sqrt{\tau}(x-6\tau\epsilon t)+2i\tau t-1\right]}{4\sqrt{\epsilon}\tau^{\frac{3}{4}}}e^{\xi_2}-(\alpha d_2+\beta d_3)e^{\xi_3},$$

$$\chi_1^{[0]}=\frac{(i-1)d_2\left[2\sqrt{\tau}(x-6\tau\epsilon t)+2i\tau t-1\right]}{4\sqrt{\epsilon}\tau^{\frac{3}{4}}}e^{\xi_2}+\alpha d_1e^{\xi_3},$$

$$\psi_1^{[0]}=\frac{(i-1)d_3\left[2\sqrt{\tau}(x-6\tau\epsilon t)+2i\tau t-1\right]}{4\sqrt{\epsilon}\tau^{\frac{3}{4}}}e^{\xi_2}+\beta d_1e^{\xi_3},$$

$$\phi_1^{[1]}=\frac{1-i}{96\tau^{\frac{1}{4}}\epsilon^{\frac{3}{2}}}[-16\tau^{\frac{3}{2}}\epsilon x^3+288\tau^{\frac{5}{2}}\epsilon^2x^2t+48\tau^{\frac{5}{2}}\epsilon xt^2-1728\tau^{\frac{7}{2}}\epsilon^3xt^2$$
$$+3456\tau^{\frac{9}{2}}\epsilon^4t^3-288\tau^{\frac{7}{2}}\epsilon^2t^3-40\epsilon\tau x^2+576\epsilon^2\tau^2xt-2016\epsilon^3\tau^3t^2$$
$$+56\tau^2\epsilon t^2-20\sqrt{\tau}\epsilon x+552\tau^{\frac{3}{2}}\epsilon^2t-3\sqrt{\tau}m_1+6\epsilon+i(-1728\tau^4\epsilon^3t^3$$
$$+576\tau^3\epsilon^2xt^2+16\tau^3\epsilon t^3-48\tau^2\epsilon x^2t-96\tau^{\frac{3}{2}}\epsilon xt+672\tau^{\frac{5}{2}}\epsilon^2t^2$$
$$-76\tau\epsilon t-3\sqrt{\tau}n_1)]e^{\xi_1},$$

$$\varphi_1^{[1]}=-\frac{2}{3}(12\tau^{\frac{3}{2}}\epsilon t-2i\tau t-\sqrt{\tau}x)(\alpha d_2+\beta d_3)e^{\xi_3}+\frac{d_1\Omega}{96\epsilon^{\frac{3}{2}}\tau^{\frac{3}{4}}}e^{\xi_2},$$

$$\chi_1^{[1]}=\frac{2}{3}\alpha d_1(12\tau^{\frac{3}{2}}\epsilon t-2i\tau t-\sqrt{\tau}x)e^{\xi_3}-\frac{d_2\Omega}{96\epsilon^{\frac{3}{2}}\tau^{\frac{3}{4}}}e^{\xi_2},$$

$$\psi_1^{[1]}=\frac{2}{3}\beta d_1(12\tau^{\frac{3}{2}}\epsilon t-2i\tau t-\sqrt{\tau}x)e^{\xi_3}-\frac{d_3\Omega}{96\epsilon^{\frac{3}{2}}\tau^{\frac{3}{4}}}e^{\xi_2},$$

……

with

$$\xi_1=\frac{1}{3}\sqrt{\tau}x+\tau\left(\frac{5}{6}i-\frac{4}{3}\epsilon\sqrt{\tau}\right)t,\quad \xi_2=\frac{1}{3}\sqrt{\tau}x-\tau\left(\frac{1}{6}i+\frac{4}{3}\epsilon\tau\right)t,$$

$$\xi_3=-\frac{2}{3}\sqrt{\tau}x-\tau\left(\frac{2}{3}i-\frac{8}{3}\sqrt{\tau\epsilon}\right)t,$$

$$\begin{aligned}\Omega=(i-1)\Big[&-16\tau^{\frac{3}{2}}\epsilon x^3+288\tau^{\frac{5}{2}}\epsilon^2x^2t+48\tau^{\frac{5}{2}}\epsilon xt^2-1728\tau^{\frac{7}{2}}\epsilon^3xt^2\\&+3456\tau^{\frac{9}{2}}\epsilon^4t^3-288\tau^{\frac{7}{2}}\epsilon^2t^3+8\epsilon\tau x^2+8\tau^2\epsilon t^2-288\epsilon^3\tau^3t^2\\&-4\sqrt{\tau}\epsilon x+360\tau^{\frac{3}{2}}\epsilon^2t-3\sqrt{\tau}m_1-6\epsilon i\Big(-1728\tau^4\epsilon^3t^3\\&+576\tau^3\epsilon^2xt^2+16\tau^3\epsilon t^3-48\tau^2\epsilon x^2t-44\tau\epsilon t+96\epsilon^2\tau^{\frac{5}{2}}t^2-3\sqrt{\tau}n_1\Big)\Big].\end{aligned}$$

It can be straightforward to calculate that the vector function $\Phi_1^{[0]}$ is a solution of the Lax pair (2–3) at $\lambda=\lambda_1=8i\sqrt{\tau\epsilon}$ and $q_1=q_1[0]$, $q_2=q_2[0]$, and $q_3=q_3[0]$. Through the formulae (11–13), the first-order localised wave solutions can be expressed as

$$q_1[1]=d_1e^{i\theta}+\frac{2\left[d_1\tau^{\frac{1}{4}}\sqrt{\epsilon}F_1e^{i\theta}-2\tau\epsilon(\alpha d_2+\beta d_3)F_2e^{\eta_1}\right]}{\tau^{\frac{1}{4}}\sqrt{\epsilon}\left(4\sqrt{\tau\epsilon}G_1e^{\eta_2}+G_2\right)},\tag{31}$$

$$q_2[1]=d_2e^{i\theta}+\frac{2\left(d_2\tau^{\frac{1}{4}}\sqrt{\epsilon}F_1e^{i\theta}+2\alpha d_1\tau\epsilon F_2e^{\eta_1}\right)}{\tau^{\frac{1}{4}}\sqrt{\epsilon}\left(4\sqrt{\tau\epsilon}G_1e^{\eta_2}+G_2\right)},\tag{32}$$

$$q_3[1]=d_3e^{i\theta}+\frac{2\left(d_3\tau^{\frac{1}{4}}\sqrt{\epsilon}F_1e^{i\theta}+2\beta d_1\tau\epsilon F_2e^{\eta_1}\right)}{\tau^{\frac{1}{4}}\sqrt{\epsilon}\left(4\sqrt{\tau\epsilon}G_1e^{\eta_2}+G_2\right)},\tag{33}$$

where

$$F_1=-4\tau x^2+48\tau^2\epsilon xt-4\tau^2t^2-144\tau^3\epsilon^2t^2+4i\tau t+1,$$
$$F_2=(-1+i)\left(12\tau^{\frac{3}{2}}\epsilon t-2i\tau t-2\sqrt{\tau}x-1\right),$$
$$G_1=\alpha^2d_1^2+\alpha^2d_2^2+2\alpha\beta d_2d_3+\beta^2d_1^2+\beta^2d_3^2,$$
$$G_2=4\tau x^2-48\tau^2\epsilon xt+144\tau^3\epsilon^2t^2+4\tau^2t^2+1.$$

The correctness of (31–33) have been directly verified by putting them back into (1). At this point, we obtain the first-order localised nonlinear waves of (1) with five free parameters d_1, d_2, d_3, α, and β. Besides, the parameters d_1, d_2, and d_3 determine the background in which the different localised waves emerge, and α, β play an important role in controlling the dynamics of these nonlinear waves. These first-order nonlinear localised wave solutions are discussed in the following six different mixed interactional cases:

(i) When $\alpha=\beta=0$, q_1, q_2, and q_3 are all proportional to each other, the first-order interactional localised waves degenerate to the first-order rogue waves. Besides, these three components have similar structures, and the first-order rogue wave is the same as the standard NLS equation [10, 11] (see Fig. 1).

(ii) When one of the two parameters α, β is zero and $d_i\neq 0$ ($i=1, 2, 3$), without loss of generality, we choose $\alpha=0$, $\beta\neq 0$. It demonstrates that q_1 and q_3 components are all the interactional solutions between a first-order RW and a breather, and the q_2 component is the interactional solution between a first-order RW and a dark soliton in Figure 2. By increasing the absolute value of β, the phenomenon that the nonlinear waves merge with each other distinctly.

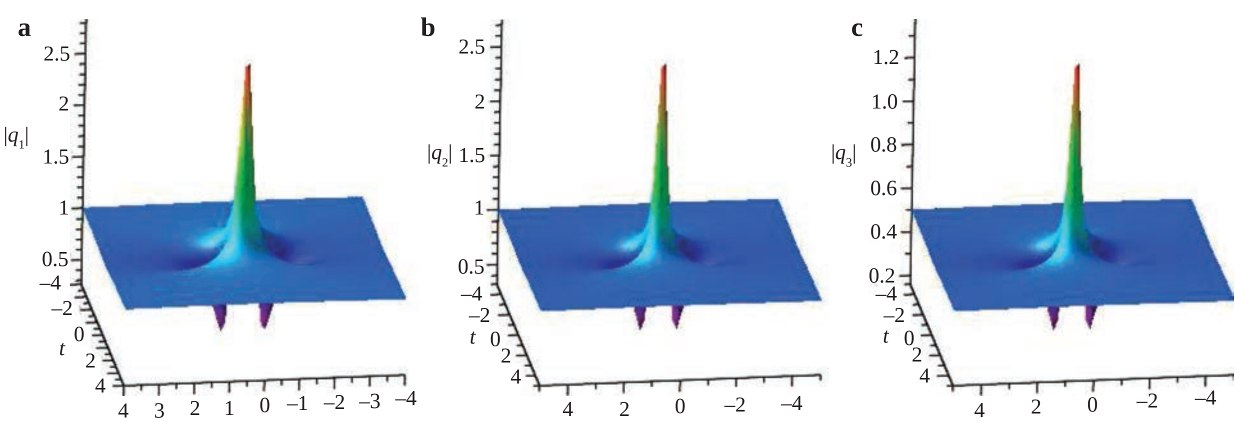

Figure 1: Evolution plot of the first-order RW of the three-component coupled Hirota equations with the parameters chosen by $d_1=1,\ d_2=-1,\ d_3=-0.5,\ \epsilon=\frac{1}{100}$: (a) q_1, (b) q_2, (c) q_3.

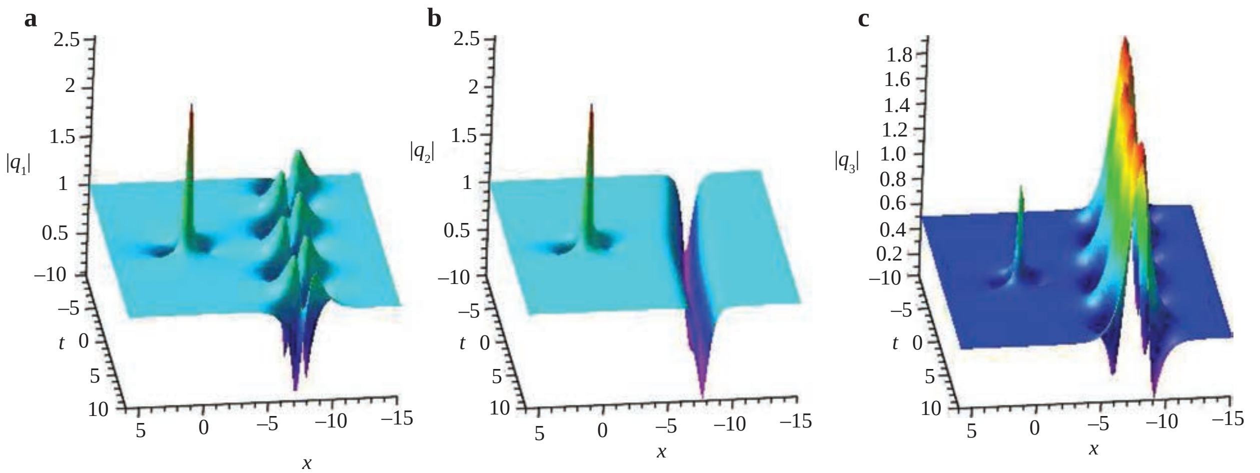

Figure 2: Evolution plot of the interactional solution between the first-order RW and one-dark soliton or one-breather in the three-component coupled Hirota equations with the parameters chosen by $d_1=1$, $d_2=-1$, $d_3=-0.5$, $\epsilon=\frac{1}{100}$, $\alpha=0$, $\beta=-\frac{1}{2000}$: (a) a first-order RW and a breather separate in q_1 component; (b) a first-order RW and a dark soliton separate in q_2 component; (c) a first-order RW and a breather separate in q_3 component.

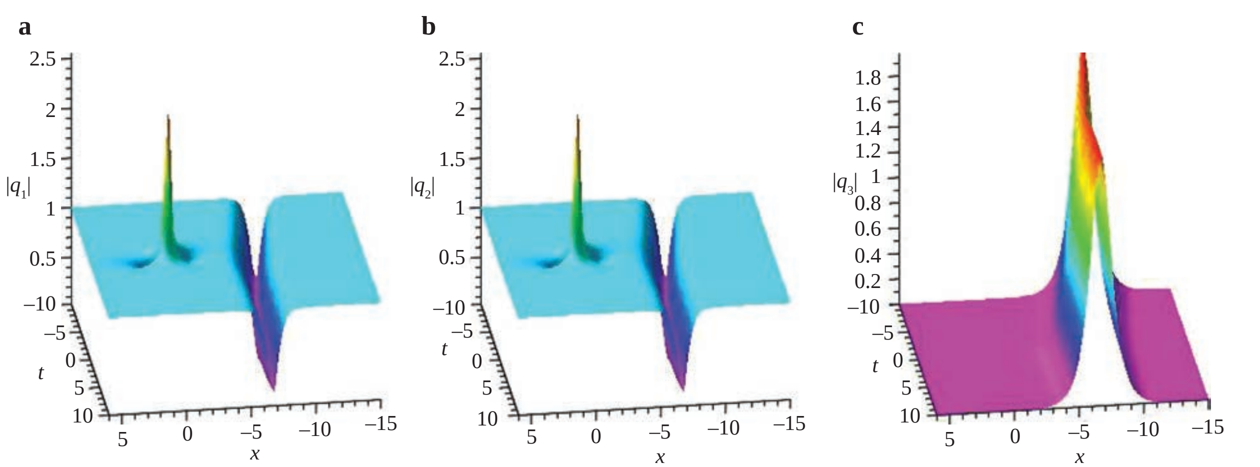

Figure 3: Evolution plot of the interactional solution between the first-order RW and one-dark soliton or one-bright soliton in the three-component coupled Hirota equations with the parameters chosen by $d_1=1$, $d_2=-1$, $d_3=0$, $\epsilon=\frac{1}{100}$, $\alpha=0$, $\beta=-\frac{1}{200}$: (a) a first-order RW and a dark soliton separate in q_1 component; (b) a first-order RW and a dark soliton separate in q_2 component; (c) a first-order RW and a bright soliton separate in q_3 component.

(iii) When $\alpha=0$, $\beta\neq 0$ and one of the three parameters d_i $(i=1, 2, 3)$ is zero, without loss of generality, we choose $d_1\neq 0$, $d_2\neq 0$, $d_3=0$. It shows that q_1 and q_2 components are all the hybrid solutions between a first-order RW and a dark soliton, and q_3 is the hybrid solution between a first-order RW and a bright soliton in Figure 3. We can find that the rogue wave cannot be easily identified in Figure 3c. At this time, the amplitude of the plane wave background in q_3 component is zero and the amplitude of the rogue wave is dependent on this background, so the rogue wave cannot be easily observed. In the same way, these nonlinear waves merge with each other by increasing the absolute value of β (see Fig. 4). Besides, the first-order RW in the interactional solutions of q_3 component can be easily found in Figure 4c by increasing the absolute value of β because the amplitude of the part of the plane wave background where the first-order RW emerges is not zero.

(iv) When $\alpha\neq 0$, $\beta\neq 0$, and one of the three parameters d_i $(i=1, 2, 3)$ is zero, without loss of generality, we set $d_1\neq 0$, $d_2\neq 0$, and $d_3=0$. Here, q_1 and q_2 components are all the interactional solutions between a first-order RW and a breather, and the q_3 component

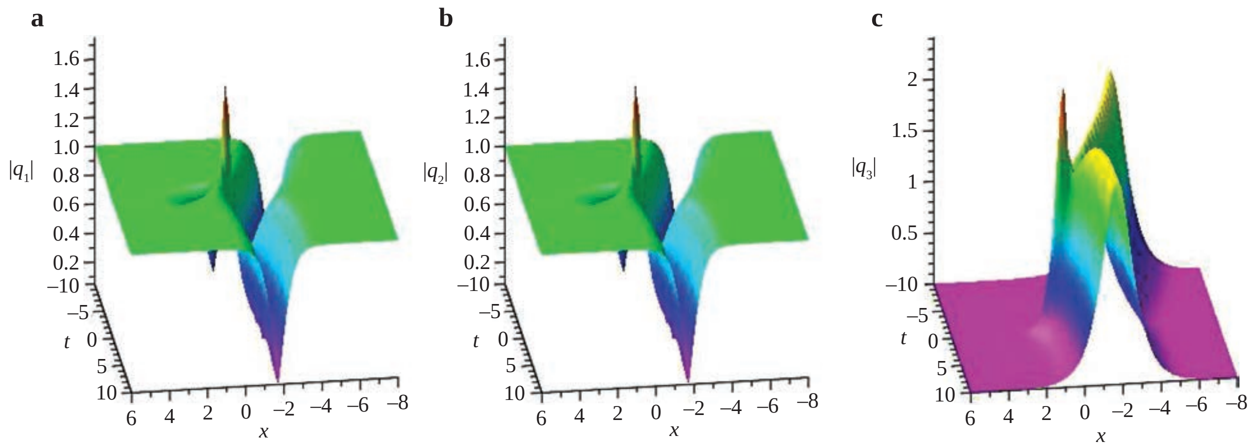

Figure 4: Evolution plot of the interactional solution between the first-order RW and one-dark soliton or one-bright soliton in the three-component coupled Hirota equations with the parameters chosen by $d_1=1$, $d_2=-1$, $d_3=0$, $\epsilon=\frac{1}{100}$, $\alpha=0$, $\beta=-5$: (a) a first-order RW merges with a dark soliton in q_1 component; (b) a first-order RW merges with a dark soliton in q_2 component; (c) a first-order RW merges with a bright soliton in q_3 component.

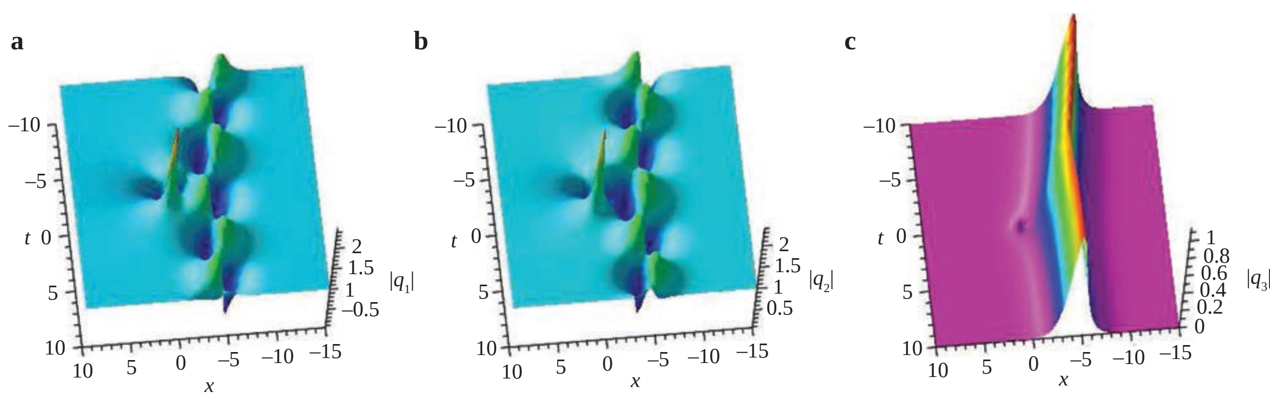

Figure 5: Evolution plot of the interactional solution between the first-order RW and one-breather or one-bright soliton in the three-component coupled Hirota equations with the parameters chosen by $d_1=1$, $d_2=-1$, $d_3=0$, $\epsilon=\frac{1}{100}$, $\alpha=\frac{1}{10}$, $\beta=-\frac{1}{10}$: (a) a first-order RW and a breather separate in q_1 component; (b) a first-order RW and a breather separate in q_2 component; (c) a first-order RW and a bright soliton separate in q_3 component.

is the interactional solution between a first-order RW and a bright soliton (see Fig. 5). Although considering the zero-amplitude background crest, the first-order RW of q_3 component in the Figure 5c is difficult to observe owing to its small amplitude. Analogously, different nonlinear waves can merge with each other by increasing the absolute values of α and β.

(v) When $\alpha\neq 0$, $\beta\neq 0$, and two of the three parameters d_i ($i=1, 2, 3$) are zero, without loss of generality, we set $d_1\neq 0$, $d_2=d_3=0$. From Figure 6, we can find that a first-order RW merges with a bright soliton in q_2 and q_3 components, and a first-order RW merges with a dark soliton in q_1 component. Figure 7 describes the explicit collision processes between a dark soliton and a first-order RW in q_1 component, a bright soliton and a first-order RW in q_2 and q_3 components, respectively. A dark soliton in q_1 component and a bright soliton in q_2 and q_3 components propagate along the positive direction of x-axis, when $t=0$, the first-order RW suddenly appears and these nonlinear waves interact with each other. At the next moment, the first-order RW disappears without a trace and the solitons continue to propagate without changing their velocities and amplitudes. The interactional process is elastic collision.

(vi) When $\alpha\neq 0$, $\beta\neq 0$, and d_i ($i=1, 2, 3$) are all not zero, the three components q_1, q_2, and q_3 are all the interactional solutions between a first-order RW and a breather in Figure 8. In the same way, increasing the

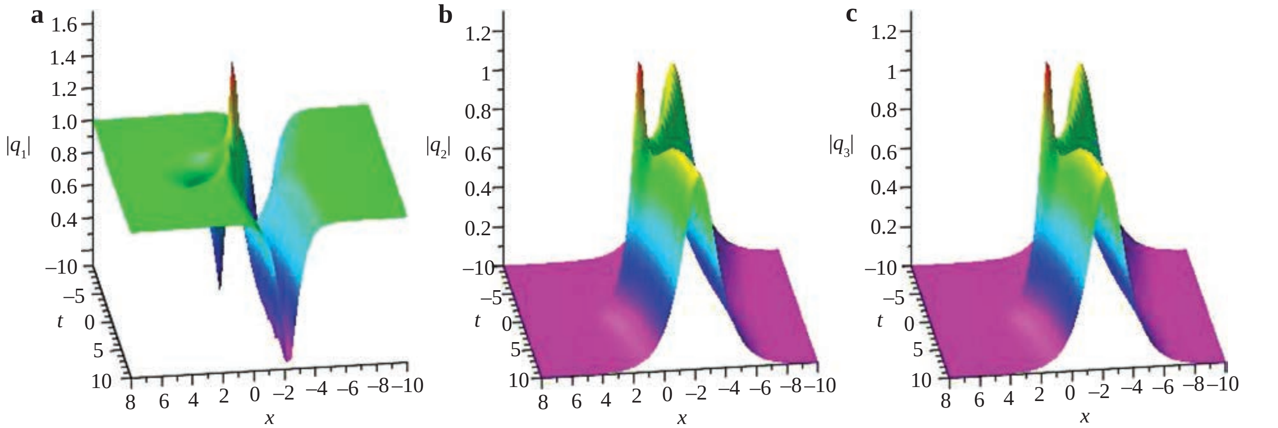

Figure 6: Evolution plot of the interactional solution between the first-order RW and one-dark soliton or one-bright soliton in the three-component coupled Hirota equations with the parameters chosen by $d_1=1$, $d_2=d_3=0$, $\epsilon=\frac{1}{100}$, $\alpha=5$, $\beta=-5$: (a) a first-order RW merges with a dark soliton in q_1 component; (b) a first-order RW merges with a bright soliton in q_2 component; (c) a first-order RW merges with a bright soliton in q_3 component q_3.

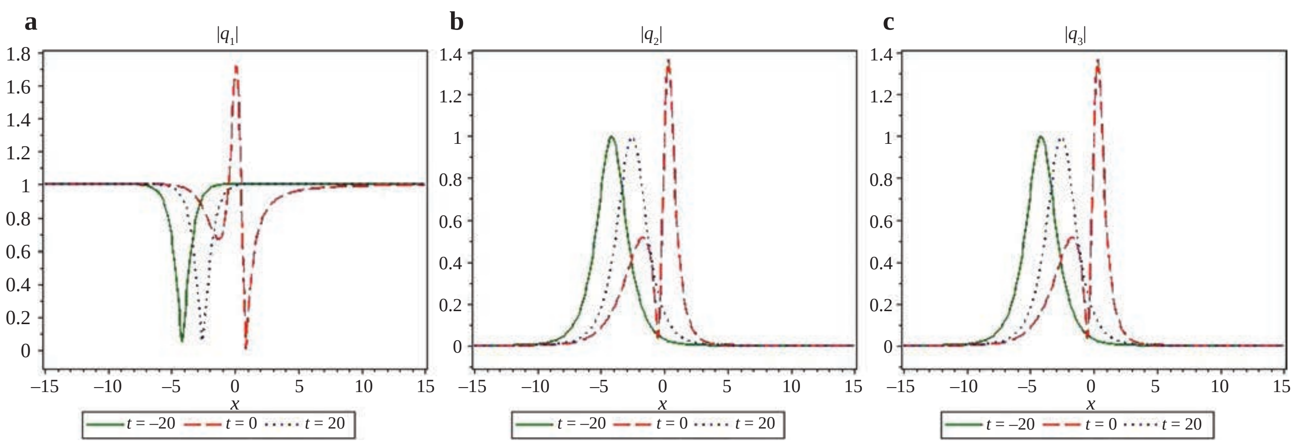

Figure 7: Plane evolution plot of the interactional process between the first-order RW and the right-going one-dark soliton or one-bright soliton in three different moments $t=-20$, $t=0$, $t=20$ in Figure 6: (a) q_1, (b) q_2, and (c) q_3.

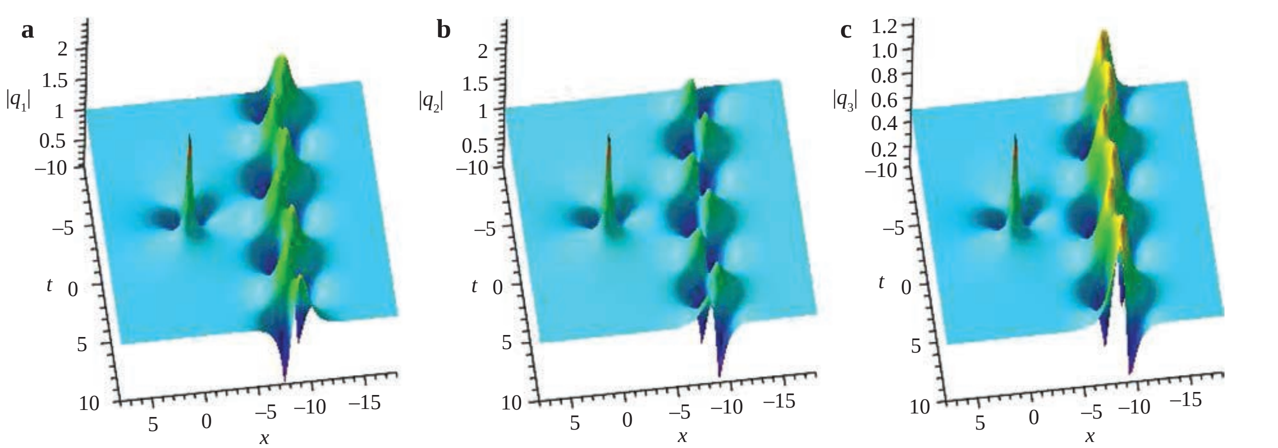

Figure 8: Evolution plot of the interactional solution between the first-order RW and one-breather in the the three-component coupled Hirota equations with the parameters chosen by $d_1=1$, $d_2=-1$, $d_3=0.5$, $\epsilon=\frac{1}{100}$, $\alpha=\frac{1}{10{,}000}$, $\beta=-\frac{1}{10{,}000}$: a first-order RW and a breather all separate in the three components (a) q_1, (b) q_2, and (c) q_3.

Table 1: Classification of the first-order localised wave solution generated by the first-step generalised DT.

d_i	q_1	q_2	q_3
$d_1\neq 0,\ d_2=d_3=0$	RW and one-dark soliton	0	RW and one-bright soliton
$d_1=0,\ d_2\neq 0,\ d_3=0$	0	RW	0
$d_1=0,\ d_2=0,\ d_3\neq 0$	RW and one-bright soliton	0	RW and one-dark soliton
$d_1\neq 0,\ d_2=0,\ d_3\neq 0$	RW and one-breather	0	RW and one-breather
$d_1\neq 0,\ d_2\neq 0,\ d_3=0$	RW and one-dark soliton	RW and one-dark soliton	RW and one-bright soliton
$d_1=0,\ d_2\neq 0,\ d_3\neq 0$	RW and one-bright soliton	RW and one-dark soliton	RW and one-dark soliton
$d_1\neq 0,\ d_2\neq 0,\ d_3\neq 0$	RW and one-breather	RW and one-dark soliton	RW and one-breather

Table 2: Classification of the first-order localised wave solutions generated by the first-step generalised DT.

d_i	q_1	q_2	q_3
$d_1\neq 0,\ d_2=d_3=0$	RW and one-dark soliton	RW and one-bright soliton	RW and one-bright soliton
$d_1=0,\ d_2\neq 0,\ d_3=0$	RW and one-bright soliton	RW and one-dark soliton	0
$d_1=0,\ d_2=0,\ d_3\neq 0$	RW and one-bright soliton	0	RW and one-dark soliton
$d_1\neq 0,\ d_2=0,\ d_3\neq 0$	RW and one-breather	RW and one-bright soliton	RW and one-breather
$d_1\neq 0,\ d_2\neq 0,\ d_3=0$	RW and one-breather	RW and one-breather	RW and one-bright soliton
$d_1=0,\ d_2\neq 0,\ d_3\neq 0$	RW and one-bright soliton	RW and one-dark soliton	RW and one-dark soliton
$d_1\neq 0,\ d_2\neq 0,\ d_3\neq 0$	RW and one-breather	RW and one-breather	RW and one-breather

Table 3: Six types of the mixed first-order localised nonlinear waves.

Types	q_i ($i=1, 2, 3$)
Type 1	Three potential functions are all first-order RW
Type 2	There are two potential functions are RW and one-breather, and another one is RW and one-dark soliton
Type 3	The two potential functions are RW and one-dark soliton, and another one is RW and one-bright soliton
Type 4	The two potential functions are RW and one-breather, and another one is RW and one-bright soliton
Type 5	The two potential functions are RW and one-bright soliton, and another one is RW and one-dark soliton
Type 6	Three potential functions are all RW and one-breather

absolute values of α and β, the first-order RW merges with a breather distinctively.

According to different values of these five free parameters α, β, and d_i ($i=1, 2, 3$), a simple classification corresponding to different mixed types of the first-order nonlinear wave solutions in the coupled system (1) can be given.

Case 1: When $\alpha=\beta=0$, these solutions q_i ($i=1, 2, 3$) are all first-order rogue waves.

Case 2: One of the two parameters α and β is zero, without loss of generality, we choose $\alpha=0$, $\beta\neq 0$. This classification is shown in Table 1.

Case 3: When $\alpha\neq 0$, $\beta\neq 0$, the classification is shown in Table 2.

Instead of considering various arrangements of the three potential functions q_1, q_2, and q_3, we define the same combination as the same type of solution. For example, Case 1 is that q_1 and q_2 are all the interactional solutions between RW and one-dark soliton, q_3 is the interactional solution between RW and one-bright soliton; and Case 2 is that q_1 is the interactional solution between RW and one-bright soliton, q_2 and q_3 are all the interactional solutions between RW and one-dark soliton, according to our definition, these two cases are the same type of solution. Six types of the mixed first-order interactional solutions can be obtained using our method in this article and these different classifications are shown in Table 3.

3.2 The Second-Order Localised Nonlinear Waves

In this section, we consider the following limit:

$$\lim_{f\to 0}\frac{T[1]|_{\lambda=8i\sqrt{\tau\epsilon(1+f^2)}}\,\Phi_1}{f^2}=\lim_{f\to 0}\frac{\left(8i\sqrt{\tau\epsilon}f^2+T_1[1]\right)\Phi_1}{f^2}$$
$$=8i\sqrt{\tau\epsilon}\Phi_1^{[0]}+T_1[1]\Phi_1^{[1]}\equiv\Phi_1[1], \qquad (34)$$

$$T_1[1]=\lambda_1 I-H[0]\Lambda_1 H[0]^{-1}=(\lambda_1-\lambda_1^*)I-(\lambda_1-\lambda_1^*)\frac{\Phi_1[0]\Phi_1[0]^\dagger}{\Phi_1[0]^\dagger\Phi_1[0]}$$
$$=(\lambda_1-\lambda_1^*)I-(\lambda_1-\lambda_1^*)\frac{\Phi_1^{[0]}\Phi_1^{[0]\dagger}}{\Phi_1^{[0]\dagger}\Phi_1^{[0]}},$$
$$=16i\sqrt{\tau\epsilon}\left(I-\frac{\Phi_1^{[0]}\Phi_1^{[0]\dagger}}{\Phi_1^{[0]\dagger}\Phi_1^{[0]}}\right), \qquad (35)$$

where $\Phi_1^{[0]}=\frac{\partial^0\Phi_1}{\partial f^0}|_{f=0}$, $\Phi_1^{[1]}=\frac{\partial^2\Phi_1}{\partial f^2}|_{f=0}$. We can arrive at a specific vector solution of Lax pair (2–3) at $q_1=q_1[1]$, $q_2=q_2[1]$, $q_3=q_3[1]$, and $\lambda=\lambda_1=8i\sqrt{\tau\epsilon}$. Through (15–29), the concrete expressions of the second-order localised nonlinear waves can be derived. However, this explicit expressions of $q_1[2]$, $q_2[2]$, and $q_3[2]$ are very tedious and complicated, their expressions of the simplest case $\alpha=\beta=0$ are only given in the following content. Here, the expressions for other cases are omitted. Besides, some dynamic properties of these solutions are discussed in detail. The validity of the expressions of q_i $(i=1, 2, 3)$ can be directly verified by placing them in (1) through Maple software. It is similar to the first-order case that we discuss the dynamic properties of these nonlinear waves in six types.

(i) $\alpha=\beta=0$ and $d_i\neq 0$ $(i=1, 2, 3)$. Choosing $d_1=1$, $d_2=-2$, $d_3=2$, $\epsilon=\frac{1}{100}$, the concrete expressions of the second-order localised waves can be given. In this case, the three components q_1, q_2, and q_3 are all proportionable to each other, and they are the second-order RW. When $m_1=n_1=0$, they are the fundamental second-order RW, whereas $m_1\neq 0$, $n_1\neq 0$, they are the second-order RW of triangular pattern (see Fig. 9).

$$q_1[2]=3e^{9it}\frac{15000it-69687t^2+8100xt-7500x^2+625}{r_1}$$
$$-2e^{9it}\frac{ip_1+p_2}{r_1r_2}, \qquad (36)$$

$$q_2[2]=-6e^{9it}\frac{15000it-69687t^2+8100xt-7500x^2+625}{r_1}$$
$$+4e^{9it}\frac{ip_1+p_2}{r_1r_2}, \qquad (37)$$

$$q_3[2]=6e^{9it}\frac{15000it-69687t^2+8100xt-7500x^2+625}{r_1}$$
$$-4e^{9it}\frac{ip_1+p_2}{r_1r_2}, \qquad (38)$$

where

$$r_1=209061t^2-24300tx+22500x^2+625,$$

$$\begin{aligned}r_2=&\,1015258328477109t^6-354022663940100t^5x\\&+368948239537500t^4x^2-77797057500000t^3x^3\\&+39707718750000t^2x^4-4100625000000tx^5\\&+1265625000000x^6+105468750000x^4\\&+75937500000x^3t-6002859375000x^2t^2\\&-1851022125000xt^3+79615779001875t^4\\&-2636718750000m_1x^3+(4271484375000m_1\\&-23730468750000n_1)x^2t+(25628906250000n_1\\&+68884804687500m_1)xt^2+(64271601562500n_1\\&-38028171093750m_1)t^3+26367187500x^2\\&-53789062500xt+909699609375t^2+219726562500m_1x\\&+(1977539062500n_1-435058593750m_1)t\\&+1373291015625m_1^2+1373291015625n_1^2+244140625,\end{aligned}$$

$$\begin{aligned}p_1=&-318620397546090000000t^6x+332053415583750000000t^5x^2\\&-70017351750000000000t^4x^3+35736946875000000000t^3x^4\\&-3690562500000000000t^2x^5+1139062500000000000tx^6\\&+913732495629398100000t^7-949218750000000x^4t\\&+683437500000000x^3t^2-1653235312500000000x^2t^3\\&-1905068362500000000xt^4+245741455378125000t^5\\&+(118652343750000000m_1+640722656250000000n_1)x^3t\\&-(192216796875000000m_1+585834082031250000n_1)t^2x^2\\&+(595333863281250000n_1+330741035156250000m_1)xt^3\\&-(174863464453125000m_1-38462987272851562500n_1)t^4\\&-791015625000000tx^2-284765625000000xt^2\\&+126597304687500000t^3-164794921875000n_1x^2\\&+(1779785156250000n_1+9887695312500000m_1)xt\\&+(44014086914062500n_1-124584960937500000m_1)t^2\\&+(30899047851562500m_1^2t+30899047851562500n_1^2)t\\&-21972656250000t-22888183593750n_1,\end{aligned}$$

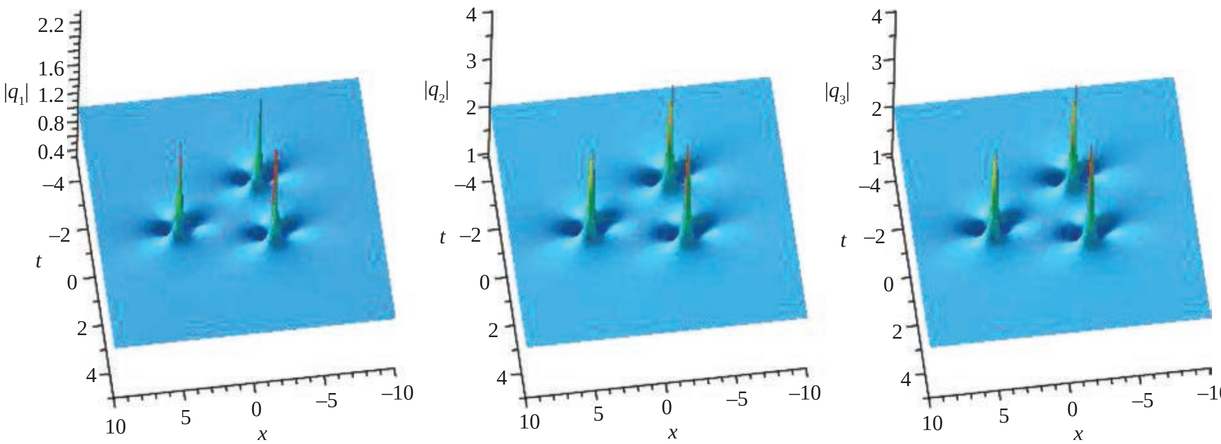

Figure 9: Evolution plot of the second-order RW of triangular pattern in the the three-component coupled Hirota equations with the parameters chosen by $d_1=1,\ d_2=-2,\ d_3=2,\ \epsilon=\frac{1}{100},\ m_1=n_1=50$: (a) q_1, (b) q_2, and (c) q_3.

$$
\begin{aligned}
p_2 = {} & -2847656250000000x^8 + 12301875000000000x^7t \\
& -12576616875000000x^6t^2 + 35726121225000000x^5t^3 \\
& -33195282797421000000t^5x^3 + 18493139276437500000t^4x^4 \\
& -10857875103042867000x^2t^6 + 98683109527974994800xt^7 \\
& -2122509214097528846 49t^8 + 316406250000000x^6 \\
& -1708593750000000tx^5 + 4594408593750000000t^2x^4 \\
& -8295154312500000000x^3t^3 + 4407181779093750000x^2t^4 \\
& -2656332241017750000xt^5 + 254814514401386 2500t^6 \\
& +593261718750000x^5m_1 + (5339355468750000n_1 \\
& -1601806640625000m_1)tx^4 - (8948759765625000m_1 \\
& +1153300781250000n_1)t^2x^3 + (16365338085937500m_1 \\
& +4137786914062500n_1)t^3x^2 - (15325210710351562500m_1 \\
& +3796204851562500n_1)t^4x + (7950207477030468750m_1 \\
& -1343668529425781250 0n_1)t^5 + 39550781250000x^4 \\
& -12339843750000x^3t + 801615234375000x^2t^2 \\
& -1807863046875000xt^3 + 1213608861070312 50t^4 \\
& +329589843750000m_1x^3 + (177978515625000m_1 \\
& -2966308593750000n_1)tx^2 + (841838378906250 00m_1 \\
& +3203613281250000n_1)xt^2 - (17575022460937500m_1 \\
& -9763901367187500 0n_1)t^3 - (30899047851562500m_1^2 \\
& +30899047851562500n_1^2 + 21972656250000)x^2 \\
& +(33370971679687500m_1^2 - 71191406250000 \\
& +33370971679687500n_1^2)xt - (287101593017578125m_1^2 \\
& +287101593017578125n_1^2 - 1032196289062500)t^2 \\
& +411987304687500m_1x - (420227050781250m_1 \\
& -2059936523437500n_1)t + 858306884765625m_1^2 \\
& +858306884765625n_1^2 - 152587890625.
\end{aligned}
$$

(ii) $\alpha=0$, $\beta\neq 0$ and $d_i\neq 0$ $(i=1, 2, 3)$. Here, q_1 and q_3 components are all the hybrid solutions between a second-order RW and two paralleled breathers, and q_2 is the hybrid solution between a second-order RW and two dark solitons (see Fig. 10). When $s_1=0$, a fundamental second-order RW and two parallel breathers separate in q_1 and q_3 components, and a fundamental second-order RW and two dark solitons separate in the q_2 component. Increasing the absolute value of β, a fundamental second-order RW merges with two breathers or two dark solitons distinctively. Although $s_1\neq 0$, we can see that the fundamental second-order RW splits into three first-order RWs and these three humps form a triangle in Figure 10.

(iii) $\alpha=0$, $\beta\neq 0$ and $d_1\neq 0$, $d_2\neq 0$, $d_3=0$. Here, q_1 and q_2 components are all the hybrid solutions between a fundamental second-order RW and two dark solitons, and q_3 is the hybrid solution between a fundamental second-order RW and two bright solitons (see Fig. 11). The fundamental second-order RW in Figure 11c are also unobservable for the same reason as the first-order case. By increasing the absolute value of β, a fundamental second-order RW merges with two dark or bright solitons. Choosing $s_1\neq 0$, the fundamental second-order RW in Figure 11 splits into three first-order RWs in Figure 12.

(iv) $\alpha\neq 0, \beta\neq 0$ and $d_1\neq 0, d_2\neq 0, d_3=0$. Here, q_1 and q_2 components are all the hybrid solutions between a second-order RW of triangular pattern and two breathers, and q_3 component is the hybrid solution between a second-order RW of triangular pattern and two bright solitons (see Fig. 13). Here, the second-order RW in q_3

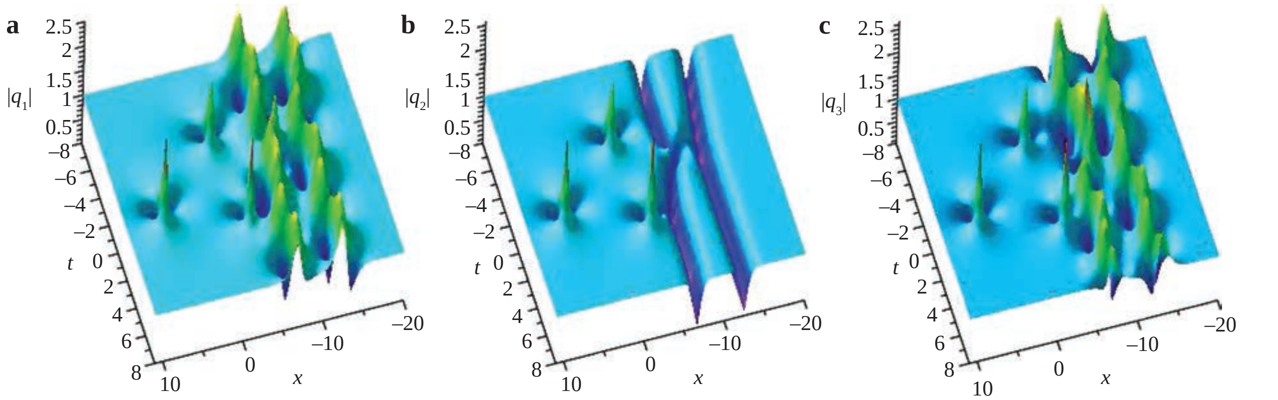

Figure 10: Evolution plot of the interactional solution between the second-order RW of triangular pattern and two-breather or two-dark soliton in the three-component coupled Hirota equations with the parameters chosen by $d_1=1,\ d_2=1,\ d_3=-1,\ \epsilon=\frac{1}{100},\ \beta=-\frac{1}{100{,}000},\ m_1=n_1=50$: (a) a second-order RW of triangular pattern and two paralleled breathers separate in q_1 component; (b) a second-order RW of triangular pattern and two dark solitons separate in q_2 component; (c) a second-order RW of triangular pattern and two paralleled breathers separate in q_3 component.

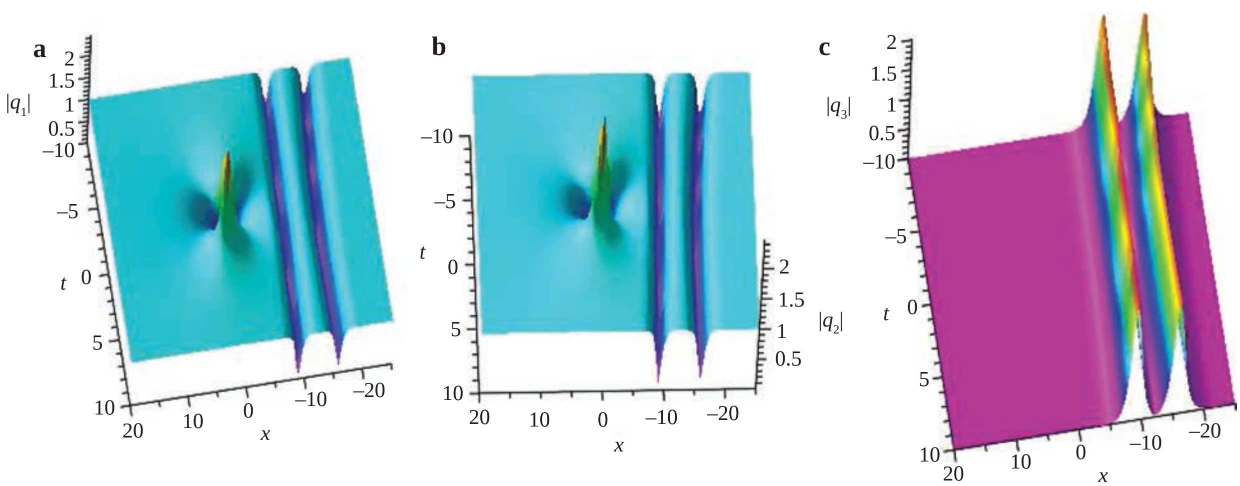

Figure 11: Evolution plot of the interactional solution between the fundamental second-order RW and two-dark or two-bright solitons in the three-component coupled Hirota equations with the parameters chosen by $d_1=1,\ d_2=-1,\ d_3=0,\ \epsilon=\frac{1}{100},\ \beta=-\frac{1}{100{,}000},\ m_1=n_1=0$: (a) a fundamental second-order RW and two dark solitons separate in q_1 component; (b) a fundamental second-order RW and two dark solitons separate in q_2 component; (c) a fundamental second-order RW and two bright solitons separate in q_3 component.

component is not discovered for the same reason as the first-order case.

(v) $\alpha\neq 0$, $\beta\neq 0$, and $d_1\neq 0$, $d_2=d_3=0$. Here, we obtain the hybrid solution between two dark solitons and a fundamental second-order RW in q_1 component, and the hybrid solutions between two bright solitons and a fundamental second-order RW in q_2 and q_3 components (see Fig. 14). In Figure 15, it is shown that the interactional process in Figure 14 is also elastic, the amplitudes and velocities of these two dark and bright solitons remain unchanged after collision.

(vi) $\alpha\neq 0$, $\beta\neq 0$, and $d_i\neq 0$ $(i=1, 2, 3)$. These three components q_1, q_2, and q_3 are all the hybrid solutions between a second-order RW of triangular pattern and two breathers (see Fig. 16). In the same way, increasing the absolute values of α and β, we can find that the second-order RW merges with the two-breather distinctively.

In the first-order localised waves, we get the concrete expressions of these interactional solutions and give the classifications in six different cases. Instead of considering various arrangements of the three potential functions q_1,

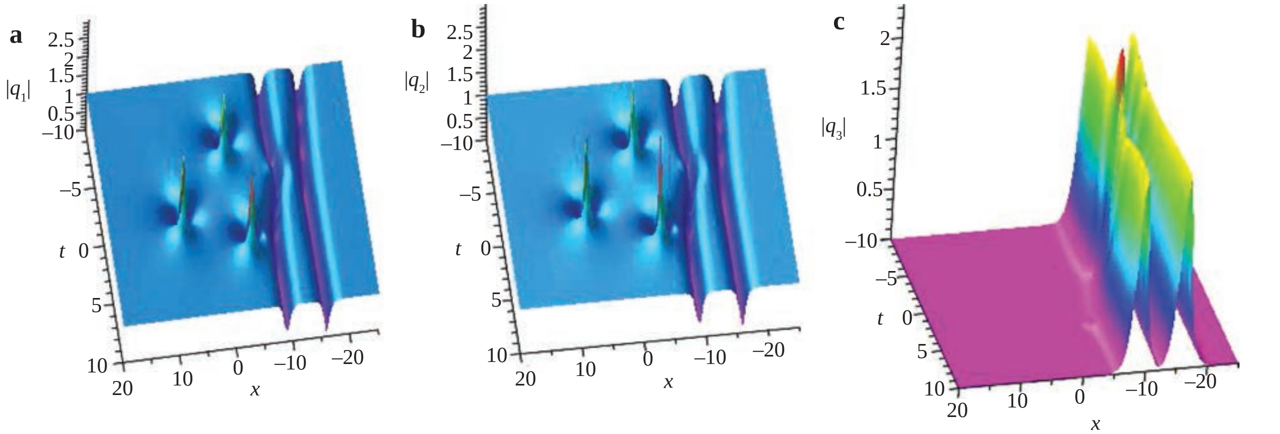

Figure 12: Evolution plot of the interactional solution between the second-order RW of triangular pattern and two-dark or two-bright solitons in the three-component coupled Hirota equations with the parameters chosen by $d_1=1$, $d_2=-1$, $d_3=0$, $\epsilon=\frac{1}{100}$, $\beta=-\frac{1}{100{,}000}$, $m_1=n_1=50$: (a) a second-order RW of triangular pattern and two dark solitons separate in q_1 component; (b) a second-order RW of triangular pattern and two dark solitons separate in q_2 component; (c) a second-order RW of triangular pattern and two bright solitons separate in q_3 component.

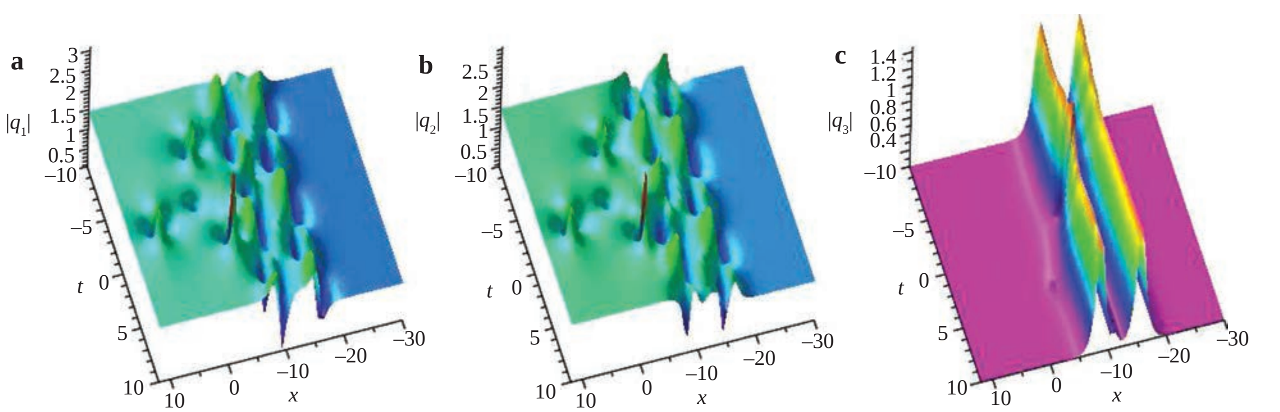

Figure 13: Evolution plot of the interactional solution between the second-order RW of triangular pattern and two-breather or two-bright solitons in the three-component coupled Hirota equations with the parameters chosen by $d_1=1$, $d_2=-1$, $d_3=0$, $\epsilon=\frac{1}{100}$, $\alpha=\frac{1}{100{,}000}$, $\beta=-\frac{1}{100{,}000}$, $m_1=n_1=50$: (a) a second-order RW of triangular pattern and two paralleled breathers separated in the q_1 component; (b) a second-order RW of triangular pattern and two paralleled breathers separate in q_2 component; (c) a second-order RW of triangular pattern and two bright solitons separate in q_3 component.

q_2, and q_3, the six mixed types first-order localised waves are obtained using our method in this article. However, the expressions of the second-order localised waves are greatly tedious and complicated, we cannot give these expressions in the general form. The classifications as the first-order ones are also not presented, and we can only give the six mixed types of interactional solutions, which are similar with the first-order case after fixing all the corresponding free parameters. Whether the second-order localised waves own more types or not, we cannot draw a firm conclusion now.

4 Conclusions

In summary, some interesting and appealing localised nonlinear waves in the three-component coupled Hirota equations were generated by the generalised DT. By choosing a periodic seed solution of (1), a peculiar vector solution of the Lax pair (2–3) is elaborately constructed. With a fixed spectral parameter and this special vector solution, we implement the Taylor series expansion of (29) at $f=0$, then construct the generalised DT of this three-component coupled Hirota equations (1). Combining the generalised

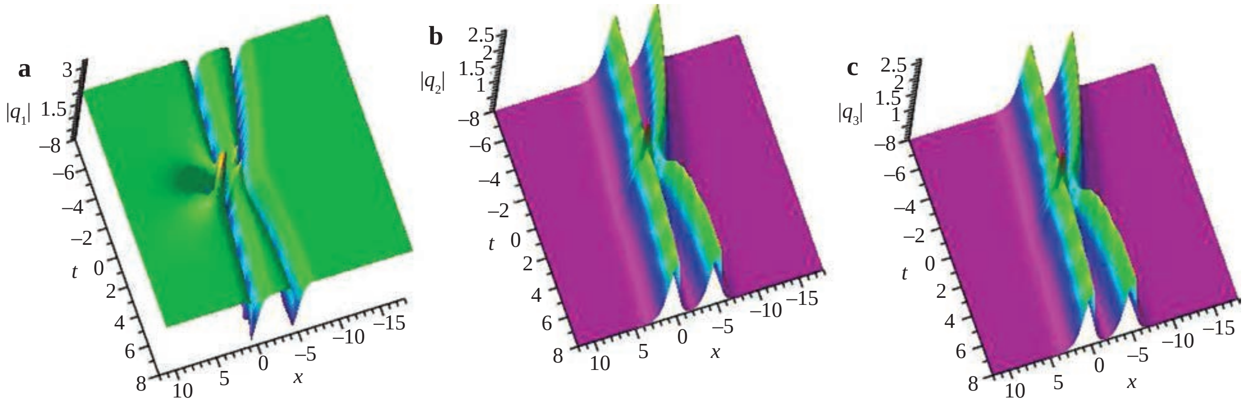

Figure 14: Evolution plot of the interactional solution between the fundamental second-order RW and two-dark solitons or two-bright solitons in the three-component coupled Hirota equations with the parameters chosen by $d_1=2,\ d_2=d_3=0,\ \epsilon=\frac{1}{100},\ \alpha=1,\ \beta=-1,\ m_1=n_1=0$: (a) a fundamental second-order RW and two dark solitons merge in q_1 component; (b) a fundamental second-order RW and two bright solitons merge in q_2 component; (c) a fundamental second-order RW and two bright solitons merge in q_3 component.

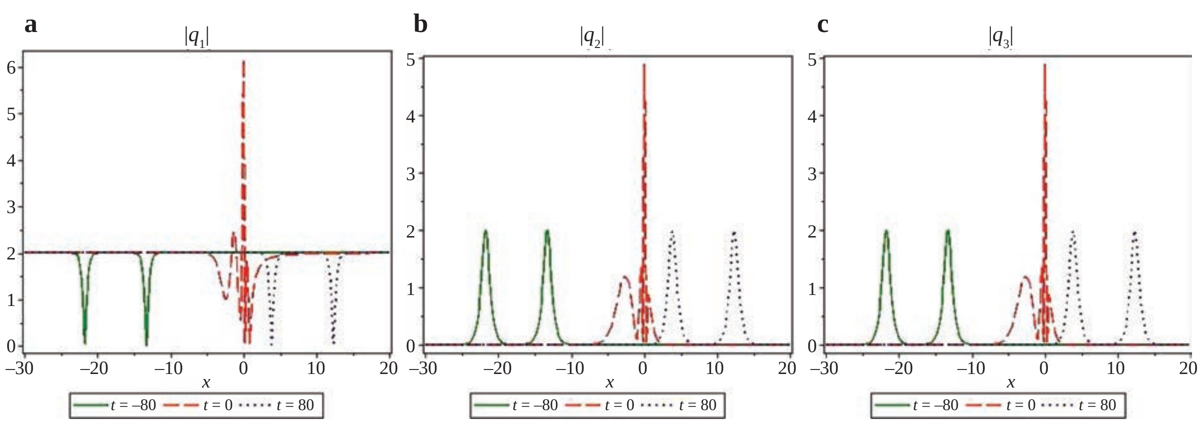

Figure 15: Plane evolution plot of the interactional process between the fundamental second-order RW and the right-going two-dark solitons or two-bright solitons at three different moments $t=-80$, $t=0$, $t=80$ in Figure 14: (a) q_1, (b) q_2, (c) q_3.

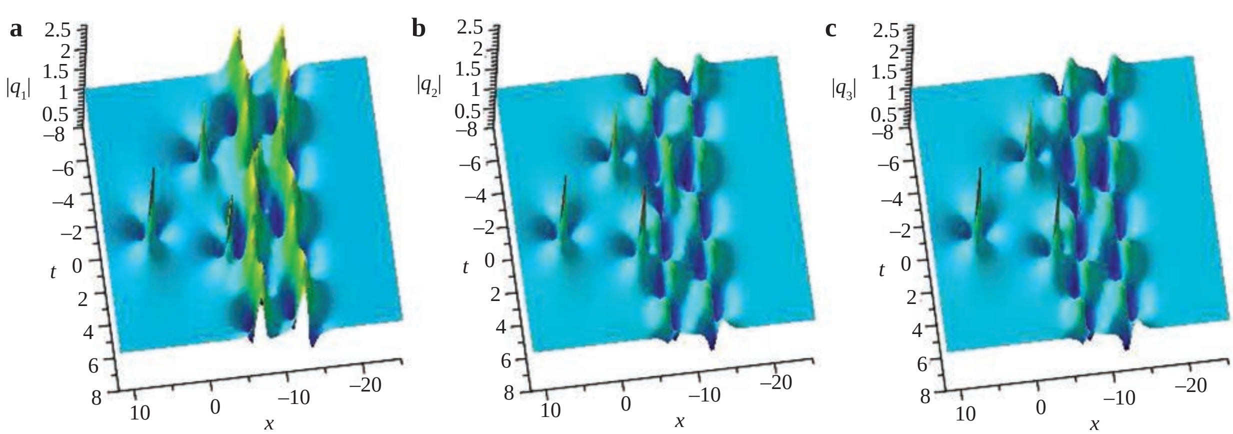

Figure 16: Evolution plot of the interactional solution between a second-order RW of triangular pattern and two-breathers in the three-component coupled Hirota equations with the parameters chosen by $d_1=1,\ d_2=1,\ d_3=-1,\ \epsilon=\frac{1}{100},\ \alpha=\frac{1}{100{,}000},\ \beta=-\frac{1}{100{,}000},\ m_1=n_1=50$: the three components are all that a second-order RW of triangular pattern separates with two parallel breathers (a) q_1, (b) q_2, and (c) q_3.

DT and the special vector solution of the Lax pair (2–3), the multiparametric and semirational solutions are constructed. The free parameter plays an important role in controlling the dynamic properties of these localised nonlinear waves, such as α, β, d_i ($i=1, 2, 3$), and s_j ($j=1, 2, \ldots, N$). The parameters α and β affect the position at which each nonlinear wave locates in the hybrid solution, e.g. separation and integration. Besides, the amplitudes d_i ($i=1, 2, 3$) of the plane wave backgrounds determine different combinations of the interactional solutions in these three components q_1, q_2, and q_3. The parameter s_j controls the structures of high-order rogue waves in the hybrid solutions.

Here, the dynamics of these interactional solutions are mainly discussed in six mixed types: (i) the hybrid solutions degenerate to the rational ones and the three components are all rogue waves; (ii) two components are hybrid solutions between rogue wave (RW) and breather (RW + breather), and one component is an interactional solution between RW and dark soliton (RW + dark soliton); (iii) two components are RW + dark soliton, and one component is RW + bright soliton; (iv) two components are RW + breather, and one component is RW + bright soliton; (v) two components are RW + dark soliton, and one component is RW + bright soliton; (vi) three components are all RW + breather.

In this article, we generalise Baronio et al.'s [31] results with other multicomponent coupled system, and thus reach the higher-order localised waves of the three-component coupled system by the generalised DT. Using the DT method, the rogue wave and dark-breather-rogue wave in the two-component coupled Hirota equations were generated by Wang and Chen [52]. Besides, in [44], Wang et al. constructed some higher-order localised waves of the two-component coupled Hirota system. Here, we extend the two-component system in [44] to three-component one [24, 39], then construct the corresponding Lax pair with 4×4 matrices. Some new combinations of these interactional solutions in the coupled system (1) are given, such as Types 2, 3, 4, and 5 in Table 3 in the first-order localised waves and the corresponding cases in the second-order localised waves cannot be constructed in the two-component coupled Hirota equations [44, 52]. Through considering both two-component (even) and three-component (odd) coupled Hirota equations, we may well understand the localised waves of the multicomponent coupled Hirota equations [24, 39]. Furthermore, we expect that these localised waves in this article will be verified in physical experiments in the future.

Acknowledgment: We would like to express our sincere thanks to our discussion group for their discussions and suggestions. This project is supported by the Global Change Research Program of China (no. 2015CB953 904), the National Natural Science Foundation of China (nos. 11275072, 11435005, and 11675054), Natural Science Foundation of Hebei Province (no. A2014210140), and the Shanghai Collaborative Innovation Center of Trustworthy Software for Internet of Things (no. ZF1213).

References

[1] N. Akhmediev, A. Ankiewicz, and M. Taki, Phys. Lett. A **373**, 675 (2009).
[2] J. M. Soto-Crespo, P. Grelu, and N. Akhmediev, Phys. Rev. E **84**, 016604 (2011).
[3] M. Shats, H. Punzmann, and H. Xia, Phys. Rev. Lett. **104**, 104503 (2010).
[4] A. Chabchoub, N. Hoffmann, M. Onorato, and N. Akhmediev, Phys. Rev. X **2**, 011015 (2012).
[5] N. Akhmediev and V. I. Korneev, Theor. Math. Phys. **69**, 1089 (1986).
[6] N. Akhmediev, J. M. Soto-Crespoand, and A. Ankiewicz, Phys. Rev. A **80**, 043818 (2009).
[7] Y. C. Ma, Stud. Appl. Math. **64**, 43 (1979).
[8] D. H. Peregrine, J. Aust. Math. Soc. Series B **25**, 16 (1983).
[9] V. I. Shrira and V. V. Geogjaev, J. Eng. Math. **67**, 11 (2010).
[10] A. Ankiewicz, D. J. Kedziora, and N. Akhmediev, Phys. Lett. A **375**, 2782 (2011).
[11] B. L. Guo, L. M. Ling, and Q. P. Liu, Phys. Rev. E **85**, 026607 (2012).
[12] P. Dubard and V. B. Matveev, Nonlinearity **26**, R93 (2013).
[13] H. Q. Zhang and J. Chen, Mod. Phys. Lett. B **30**, 1650106 (2016).
[14] H. Q. Zhang, S. S. Yuan, and Y. Wang, Mod. Phys. Lett. B **30**, 1650208 (2016).
[15] H. Q. Zhang, X. L. Liu, and L. L. Wen, Z. Naturforsch. A **71**, 2, 95 (2016).
[16] B. L. Guo, L. M. Ling, and Q. P. Liu, Stud. Appl. Math. **130**, 317 (2013).
[17] S. W. Xu, J. S. He, and L. H. Wang, J. Phys. A Math. Theor. **44**, 305203 (2011).
[18] L. Wang, Y. J. Zhu, Z. Z. Wang, F. H. Qi, and R. Guo, Commun. Nonlinear. Sci. Numer. Simul. **33**, 218 (2016).
[19] L. L. Wen and H. Q. Zhang, Nonlinear Dyn. **86**, 877 (2016).
[20] Y. Ohta and J. K. Yang, Phys. Rev. E **86**, 036604 (2012).
[21] Y. S. Tao and J. S. He, Phys. Rev. E **85**, 026601 (2012).
[22] X. Wang, B. Yang, Y. Chen, and Y. Q. Yang, Phys. Scr. **89**, 095210 (2014).
[23] L. M. Ling, B. F. Feng, and Z. N. Zhu, Physica D **327**, 13 (2016).
[24] U. Bandelow and N. Akhmediev, Phys. Lett. A **376**, 1558 (2012).
[25] L. C. Zhao and J. Liu, J. Opt. Soc. Amer. A **29**, 3119 (2012).
[26] L. M. Ling, L. C. Zhao, and B. L. Guo, Nonlinearity **28**, 3243 (2015).
[27] G. Mu, Z. Y. Qin, and R. Grimshaw, Siam. J. Appl. Math. **75**, 1 (2015).
[28] X. Wang and C. Liu, Superlattices Microstruct. **107**, 299 (2017).
[29] L. M. Ling, L. C. Zhao, and B. L. Guo, Commun. Nonlinear. Sci. Numer. Simul. **32**, 285 (2016).
[30] J. S. He, S. W. Xu, K. Porsezian, Y. Cheng, and P. T. Dinda, Phys. Rev. E **93**, 062201 (2016).

[31] X. Wang and C. Liu, arXiv:1606.09323 (2016).
[32] X. Wang, Y. Q. Li, F. Huang, and Y. Chen, Commun. Nonlinear. Sci. Numer. Simul. **20**, 434 (2015).
[33] X. Wang, J. L. Cao, and Y. Chen, Phys. Scr. **90**, 105201 (2015).
[34] F. Baronio, A. Degasperis, M. Conforti, and S. Wabnitz, Phys. Rev. L **109**, 044102 (2012).
[35] B. Ren and J. Lin, Z. Naturforsch. A **7**, 539 (2015).
[36] B. Ren and J. Lin, Z. Naturforsch. A **71**, 557 (2016).
[37] J. G. Rao, Y. B. Liu, C. Qian, and J. S. He, Z. Naturforsch. A **72** (2017).
[38] S. G. Bindu, A. Mahalingam, and K. Porsezian, Phys. Lett. A **286**, 321 (2001).
[39] H. Q. Zhang and S. S. Yuan, Commun. Nonlinear Sci. Numer. Simul. **51**, 124 (2017).
[40] B. L. Guo and L. M. Ling, Chin. Phys. Lett. **28**, 110202 (2011).
[41] B. F. Feng, Physica D **297**, 62 (2015).
[42] K. Porsezian, P. S. Sundaram, and A. Mahalingam, Phys. Rev. E **50**, 1543 (1994).
[43] R. S. Tasgal and M. J. Potasek, J. Math. Phys. **33**, 1208 (1992).
[44] X. Wang, Y. Q. Li, and Y. Chen, Wave Motion **51**, 1149 (2014).
[45] H. Q. Zhang and S. S. Yuan, Nonlinear Dyn. **89**, 531 (2017).
[46] X. Wang, B. Yang, Y. Chen, and Y. Q. Yang, Chin. Phys. Lett. **31**, 090201 (2014).
[47] X. Wang, C. Liu, and L. Wang, J. Math. Anal. Appl. **449**, 1534 (2017).
[48] T. Xu and Y. Chen, Chin. Phys. B **25**, 090201 (2016).
[49] V. B. Matveev and M. A. Salle, Darboux Transformations and Solitons, Springer, Berlin 1991.
[50] M. J. Ablowitz and H. Segur, Solitons and the Inverse Scattering Transform, SIAM, Philadelphia 1981.
[51] C. H. Gu, H. S. Hu, and Z. X. Zhou, Darboux Transformations in Integrable Systems: Theory and their Applications to Geometry, Springer-Verlag, New York 2005.
[52] X. Wang and Y. Chen, Chin. Phys. B **23**, 070203 (2014).